

Title	Assessing charge contribution from thermally treated Ni foam as current collectors for Li-ion batteries
Authors	Geaney, Hugh; McNulty, David; O'Connell, John; Holmes, Justin D.; O'Dwyer, Colm
Publication date	2016-07-22
Original Citation	Geaney, H., McNulty, D., O'Connell, J., Holmes, J. D. & O'Dwyer, C. (2016) 'Assessing charge contribution from thermally treated Ni Foam as current collectors for Li-ion batteries', Journal of the Electrochemical Society, 163(8), pp. A1805-A1811. doi: 10.1149/2.0071609jes
Type of publication	Article (peer-reviewed)
Link to publisher's version	<a href="http://jes.ecsdl.org/content/current - 10.1149/2.0071609jes">http://jes.ecsdl.org/content/current - 10.1149/2.0071609jes</a>
Rights	© The Author(s) 2016. Published by ECS. This is an open access article distributed under the terms of the Creative Commons Attribution Non-Commercial No Derivatives 4.0 License (CC BY-NC-ND, <a href="http://creativecommons.org/licenses/by-nc-nd/4.0/">http://creativecommons.org/licenses/by-nc-nd/4.0/</a> ), which permits non-commercial reuse, distribution, and reproduction in any medium, provided the original work is not changed in any way and is properly cited. For permission for commercial reuse, please email: <a href="mailto:oa@electrochem.org">oa@electrochem.org</a> . - <a href="http://creativecommons.org/licenses/by-nc-nd/4.0/">http://creativecommons.org/licenses/by-nc-nd/4.0/</a>
Download date	2024-04-19 15:12:45
Item downloaded from	<a href="https://hdl.handle.net/10468/3138">https://hdl.handle.net/10468/3138</a>



# UCC

**University College Cork, Ireland**  
Coláiste na hOllscoile Corcaigh



## Assessing Charge Contribution from Thermally Treated Ni Foam as Current Collectors for Li-Ion Batteries

Hugh Geaney,<sup>a,b,=</sup> David McNulty,<sup>a,b,=,\*</sup> John O'Connell,<sup>a,b,c</sup> Justin D. Holmes,<sup>a,b,c</sup> and Colm O'Dwyer<sup>a,b,d,\*,z</sup>

<sup>a</sup>Department of Chemistry, University College Cork, Cork T12 YN60, Ireland

<sup>b</sup>Tyndall National Institute, Lee Maltings, Cork T12 R5CP, Ireland

<sup>c</sup>AMBER@CRANN, Trinity College Dublin, Dublin D02 DA31, Ireland

<sup>d</sup>Micro-Nano Systems Centre, Tyndall National Institute, Lee Maltings, Cork T12 R5CP, Ireland

In this report we have investigated the use of Ni foam substrates as anode current collectors for Li-ion batteries. As the majority of reports in the literature focus on hydrothermal formation of materials on Ni foam followed by a high temperature anneal/oxidation step, we probed the fundamental electrochemical responses of as received Ni foam substrates and those subjected to heating at 100°C, 300°C and 450°C. Through cyclic voltammetry and galvanostatic testing, it is shown that the as received and 100°C annealed Ni foam show negligible electrochemical activity. However, Ni foams heated to higher temperature showed substantial electrochemical contributions which may lead to inflated capacities and incorrect interpretations of CV responses for samples subjected to high temperature anneals. XRD, XPS and SEM analyses clearly illustrate that the formation of electrochemically active NiO nanoparticles on the surface of the foam is responsible for this behavior. To further investigate the contribution of the oxidized Ni foam to the overall electrochemical response, we formed Co<sub>3</sub>O<sub>4</sub> nanoflowers directly on Ni foam at 450°C and showed that the resulting electrochemical response was dominated by NiO after the first 10 charge/discharge cycles. This report highlights the importance of assessing current collector activity for active materials grown on transition metal foam current collectors for Li-ion applications.

© The Author(s) 2016. Published by ECS. This is an open access article distributed under the terms of the Creative Commons Attribution Non-Commercial No Derivatives 4.0 License (CC BY-NC-ND, <http://creativecommons.org/licenses/by-nc-nd/4.0/>), which permits non-commercial reuse, distribution, and reproduction in any medium, provided the original work is not changed in any way and is properly cited. For permission for commercial reuse, please email: [oa@electrochem.org](mailto:oa@electrochem.org). [DOI: 10.1149/2.0071609jes] All rights reserved.

Manuscript submitted April 7, 2016; revised manuscript received May 18, 2016. Published June 22, 2016.

Lithium-ion batteries have found widespread use in portable electronic devices due to their improved performance in comparison with other battery chemistries (e.g. lead-acid, NiMH etc.).<sup>1-4</sup> Stimulated by the need for improved batteries for more demanding applications, the field has seen a wave of interest in the development of novel materials for every component of the battery (anode, cathode, current collectors and electrolytes).<sup>5-10</sup> Practically all literature studies focused on the development of materials for Li-ion batteries report specific capacities primarily in terms of mAhg<sup>-1</sup>.<sup>11-13</sup> While the use of common specific capacity units allows different material systems to be compared quickly, it often means that important considerations for real-world applications are ignored. For example, materials with low tap densities or a high degree of porosity can lead to electrodes which exhibit fantastic capacities in terms of mAhg<sup>-1</sup> but poor mass loadings and thus areal/volumetric capacities which are unsuited to real-world devices. This is particularly true for nanoscale materials which often lead to sub-mg level electrode mass loadings. In fact, it is well established that materials tend to perform better when using low mass loadings,<sup>14-17</sup> making the concept of using low mass loadings particularly attractive in terms of maximizing the calculated capacity in terms of mAhg<sup>-1</sup>. Given that the merits of materials are often assessed solely on the specific capacity (in terms of mAhg<sup>-1</sup>), it is crucial that the specific capacity values calculated for a system is a genuine representation of the material being assessed.

We have recently discussed the concept of electrochemically active current collectors which can give artificially inflated specific capacity values.<sup>18</sup> In that case, carbon based supports were shown to participate in the discharge chemistry of Li-O<sub>2</sub> batteries. Due to the disparity in mass between the much heavier (electrochemically active) current collector and the lighter added active material, when capacity values were calculated in the conventional manner (in terms of mAhg<sup>-1</sup>) by only factoring in the added material, the capacities were highly inflated (by up to a factor of 10). The issue of under-estimation of the mass contributing to the electrochemical response can be further

exacerbated if using specific currents (i.e. if currents used are based on mA/g), as the applied current used will not factor in contributions from the ignored electrochemically active components.

Among the different possible current collector substrates for Li-ion applications, a wide range of different foams (e.g. Cu, Ni, stainless steel), meshes, metal foils (Al, Cu, stainless steel, Ti etc.) and fabrics have been explored.<sup>19-25</sup> Ni foam has attracted significant attention as a Li-ion current collector with the majority of reports investigating binder-free, transition metal oxide based conversion mode alloy materials grown directly on the current collector.<sup>26-28</sup> These reports typically incorporate a hydrothermal step followed by a high temperature oxidation step.<sup>29-31</sup> While this latter step is required to oxidize the transition metal precursor, it may also result in unquantified oxidation of the metal current collector. This may be problematic as the metal oxides of the majority of possible metal current collectors (e.g. NiO,<sup>32-34</sup> CuO,<sup>35,36</sup> Fe<sub>3</sub>O<sub>4</sub><sup>37</sup>) are well established Li-ion active anode materials. Oxide interfaces may also reduce electronic conductivity of the electrode or lead to delamination of active materials from the substrate surface. In fact, a number of studies have purposefully investigated the formation of electrochemically active phases of metal oxides from the corresponding metal foams/foils (i.e. NiO growth on Ni and CuO growth on Cu) usually by simple thermal treatments to create anodes for Li-ion batteries.<sup>38-42</sup> However, in the case of hydrothermally formed materials, it remains important to be able to quantify the contribution of the heated current collectors to the result electrochemical responses to ensure that the reported specific capacities and fundamental responses (CVs etc.) are correctly analyzed.

In this report we assess the use of Ni foam as a current collector substrate for Li-ion anode applications. We investigate the formation of NiO on the current collector surface upon heating to temperatures, which are commonly used in the formation of active materials (300°C and 450°C) and contrast their electrochemical responses with as received Ni foam and Ni foam heated to 100°C (a temperature at which slurry based electrodes would typically be heated to remove solvents). We show clearly that the formation of electrochemically active NiO occurs at temperatures as low as 300°C and is particularly pronounced at 450°C. As a model system, Co<sub>3</sub>O<sub>4</sub> nanoflowers (NFs) were also grown at 450°C via a hydrothermal approach on Ni foam to

<sup>=</sup>These authors contributed equally to this work.

\*Electrochemical Society Member.

<sup>z</sup>E-mail: [c.odwyer@ucc.ie](mailto:c.odwyer@ucc.ie)

assess the comparative contributions of the NFs and oxidized Ni foam to the observed electrochemical responses. The findings illustrate that extreme caution is required in determining the specific capacity for transition metal based, conversion mode anode materials if they are formed on heated metal foams.

### Experimental

Ni foam was purchased from MTI Corporation (EQ-bcnf-16m, 1.6 mm thickness). 1 cm<sup>2</sup> pieces of Ni foam samples were cut, rinsed in acetone and ethanol and then allowed to dry in air, at room temperature. Samples prepared in this manner represented the “as received” Ni foam. Cleaned Ni foam samples were heated in air, in an oven to 100, 300 and 450°C for 12 hours at a ramp rate of 10°C/min. Co<sub>3</sub>O<sub>4</sub> NFs were synthesized on Ni Foam using a modified version of the method adopted by Leng et al.<sup>43</sup> 1.0 mM cobalt nitrate (Co(NO<sub>3</sub>)<sub>2</sub>·6H<sub>2</sub>O), 2.3 mM ammonium fluoride (NH<sub>4</sub>F), 5 mM carbamide (CO(NH<sub>2</sub>)<sub>2</sub>) and 3.0 mM hexadecyl trimethyl ammonium bromide (CTAB) were dissolved in 60 mL deionized (DI) water and transferred to a Teflon lined, stainless steel autoclave. 1 cm<sup>2</sup> substrates of Ni foam were rinsed in acetone and placed in the solution. The autoclave was sealed and maintained at 120°C for 12 hours. The substrates were removed, rinsed with DI water and then annealed at 450°C for 12 hours.

XRD analysis was performed using a Phillips Xpert PW3719 diffractometer using Cu K $\alpha$  radiation. (Cu K $\alpha$ ,  $\lambda$  = 0.15418 nm, operation voltage 40 kV, current 40 mA). XPS spectra were acquired on an Oxford Applied Research Escabase XPS system equipped with a CLASS VM 100 mm mean radius hemispherical electron energy analyzer with multichannel detectors in an analysis chamber with a base pressure of  $5.0 \times 10^{-10}$  mbar. Survey scans were recorded between 0 and 1400 eV with a step size of 0.7 eV, dwell time of 0.5 s, and pass energy of 100 eV. Core level scans were acquired with a step size of 0.1 eV, dwell time of 0.5 s, and pass energy of 20 eV averaged over 10 scans. A non-monochromated Al K $\alpha$  X-ray source at 200 W power was used for all scans. All spectra were acquired at a takeoff angle of 90° with respect to the analyzer axis and were charge corrected with respect to the C 1s photoelectric line. Data was processed using CasaXPS software where a Shirley background correction was employed and peaks were fitted to Voigt profiles. SEM analysis was performed using an FEI Quanta 650 FEG high resolution SEM at an accelerating voltage of 10 kV. All electrochemical results presented in this report were performed using a BioLogic VSP potentiostat/galvanostat. The electrochemical properties of heated Ni foam samples and Co<sub>3</sub>O<sub>4</sub> NFs prepared on Ni foam were investigated in a half cell configuration against a pure Li counter electrode in a two electrode, stainless steel split cell (a coin cell assembly that can be disassembled for post-mortem analysis). The electrolyte consisted of a 1 mol dm<sup>-3</sup> solution of lithium hexafluorophosphate salts in a 1:1 (v/v) mixture of ethylene carbonate in dimethyl carbonate +3 wt% vinylene carbonate. The separator used in all split cell tests was a glass fiber separator (El-Cell ECC1-01-0012-A/L, 18 mm diameter, 0.65 mm thickness). Cyclic voltammetry was performed using a scan rate of 0.2 mV s<sup>-1</sup> in a potential window of 3.0–0.01 V. Galvanostatic cycling was performed using a constant current of  $\pm 500 \mu\text{A}$  in a potential window of 3.0–0.01 V.

### Results and Discussion

XRD patterns for as received and heat treated Ni foam samples and Co<sub>3</sub>O<sub>4</sub> NFs prepared on Ni foam are presented in Figure 1. The as received Ni foam has three strong reflections at 44.51, 51.85 and 76.37°, corresponding to the (111), (200) and (220) reflections for cubic Ni (JCPDS No. 004–0850) with an *Fm-3m* space group. The Ni foam sample heated to 450°C has three additional peaks at 37.25, 43.28 and 62.88°, corresponding to the (111), (200) and (220) reflections for cubic NiO (JCPDS No. 047–1049) with an *Fm-3m* space group. This suggests that as the Ni foam is heated to higher temperatures the amount of NiO on the surface of the Ni foam increases. Any oxide layer that forms on the Ni foam from heating to 100 and 300°C may

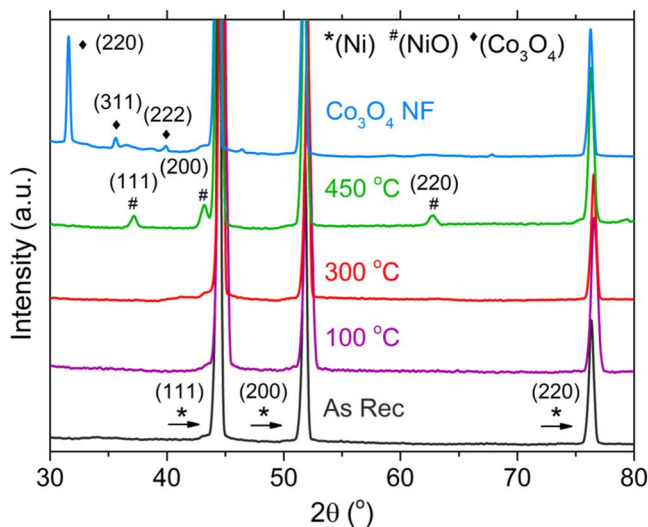


**Figure 1.** XRD patterns for as received Ni foam, Ni foam heated to 100, 300 and 450°C in air and a Co<sub>3</sub>O<sub>4</sub> NF sample which was prepared on Ni foam.

not be substantial enough for it to be detected in the corresponding XRD patterns. This will be discussed in further detail when the XPS spectra for heated Ni foam samples are compared. The XRD pattern for the cobalt oxide NFs prepared on Ni foam confirms that they are pure fcc Co<sub>3</sub>O<sub>4</sub> (JCPDS No. 42–1467). The reflections associated with NiO are not clearly seen in the XRD pattern for the Co<sub>3</sub>O<sub>4</sub> NFs prepared on Ni foam. As will be discussed, in the SEM images of the Co<sub>3</sub>O<sub>4</sub> NFs shown in Figures 3e, 3j and in greater detail in Figure S2, the NFs are quite large with diameters >10  $\mu\text{m}$  also the branches of the Ni foam are well decorated with the NFs. In contrast to this the NiO nanoparticles observed in Figure 3i are much smaller (on the scale of  $\sim 50$  nm). Consequently, the relative intensities of the Co<sub>3</sub>O<sub>4</sub> reflections may be much higher than the intensity of the NiO peaks and therefore they may be obscured in the resultant XRD pattern. The XRD pattern for Co<sub>3</sub>O<sub>4</sub> NFs prepared on Ni foam in a highlighted range from 35–43.7° is shown in Figure S1. The XRD pattern in this range is likely a convolution of the XRD patterns for Co<sub>3</sub>O<sub>4</sub> and NiO. There is a shoulder on a larger peak at  $\sim 43.2^\circ$  which may correspond to the (200) reflection for cubic NiO.

XPS analysis was performed on the various Ni foam samples to investigate their surface chemistry. The high resolution spectra for the as received, heated to 100°C, 300°C and 450°C Ni foam samples are presented in Figures 2a–2d respectively. The as received Ni foam shows multiple peaks in the Ni 2p<sub>3/2</sub> ( $\sim 855$  eV) and Ni 2p<sub>1/2</sub> ( $\sim 874$  eV) core regions and their satellites with similar peak locations reported by Grden et al. for Ni foam.<sup>44</sup> Furthermore, the Ni 2p<sub>3/2</sub> region can be subdivided into two primary peaks, which are consistent with the presence of metallic Ni at 852.9 eV and Ni<sup>2+</sup> at 854.5 eV.<sup>45</sup> The magnitude of the oxide related peak (higher energy peak) is larger for each of the samples investigated suggesting a primarily oxide-based surface chemistry for all of the samples within the probing depth of the analysis. We note that the peak location for Ni<sup>3+</sup> at 855.8 eV is extremely close to the value for Ni<sup>2+</sup> (854.5 eV) and as a result, we probed the O 1s region to investigate the nature of the oxide on the surface as a function of heat-treatment.

The high resolution spectra of the various samples for the O 1s core region (Figures 2e–2f) reflect the changes in surface chemistry upon heating more clearly. The peak at 532 eV for each of the samples is indicative of inherent Ni<sub>2</sub>O<sub>3</sub> surface passivation.<sup>45,46</sup> For the as received and 100°C samples, this peak is dominant with a smaller contribution from a lower binding energy peak at  $\sim 529$  eV. This peak is consistent with the presence of NiO and is seen to increase substantially at 300°C and is the dominant peak for the sample heat

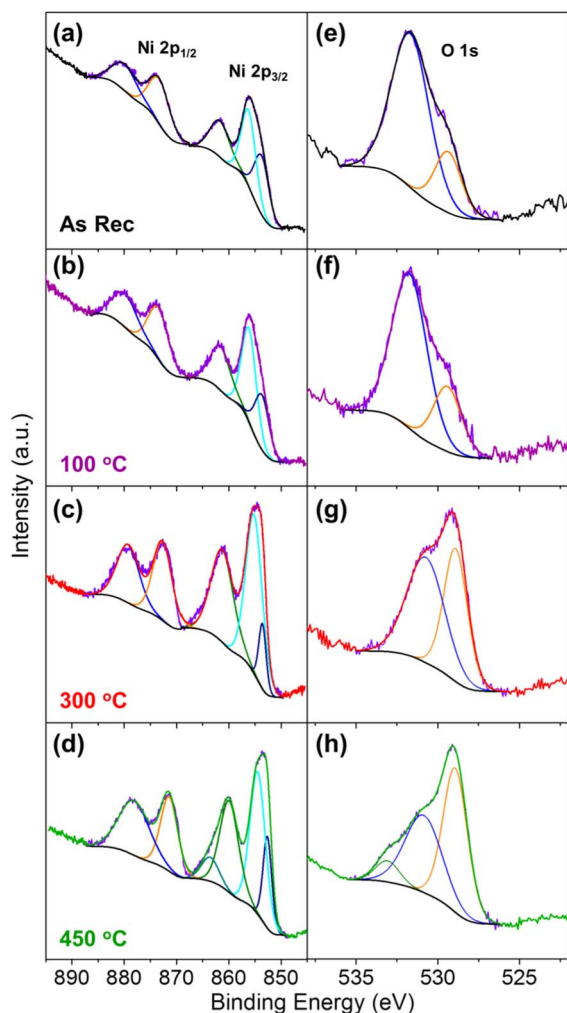


**Figure 2.** XPS spectra of the Ni 2p region for (a) as received Ni foam, Ni foam heated to (b) 100 °C, (c) 300 °C and (d) 450 °C. XPS spectra the O 1s region for (e) as received Ni Foam, Ni foam heated to (f) 100 °C, (g) 300 °C and (h) 450 °C.

treated at 450 °C. The formation of NiO upon heating is also consistent with the XRD data presented in Figure 1.

SEM analysis was used to investigate the structure of the various Ni foam samples in light of the findings from XPS and XRD analysis. Both the as received and 100 °C samples showed similarly smooth surfaces with large grains visible at low magnification (Figures 3a, 3b respectively). At higher magnification, no nanoscale surface features were evident (Figures 3f, 3g). In contrast, the Ni foam surfaces annealed at higher temperature showed markedly different surface morphologies. While the large grains were still discernible at low magnification, widespread particle formation led to a noticeably rougher surface for the sample heated to 300 °C (Figure 3c). Higher magnification images shown in (Figure 3h) revealed the presence of nanoscale particles across the surface. Similar nanoparticles were also clearly evident across the surface of the sample heated to 450 °C (Figure 3d) with a higher magnification image showing that the average particle size was larger than those seen at 300 °C (Figure 3i). Taken with the findings from XRD and XPS analysis presented in Figures 1 and 2, it is clear that heating of the Ni foam to 300 °C leads to the widespread formation of NiO nanoparticles on the surface with an increase in heating temperature to 450 °C leading to larger NiO nanoparticles. SEM images of Co<sub>3</sub>O<sub>4</sub> NFs prepared on Ni foam are shown in Figures 3e, 3j with additional images provided in Figure S2. The hydrothermally grown Co<sub>3</sub>O<sub>4</sub> sample consists of nanowires of

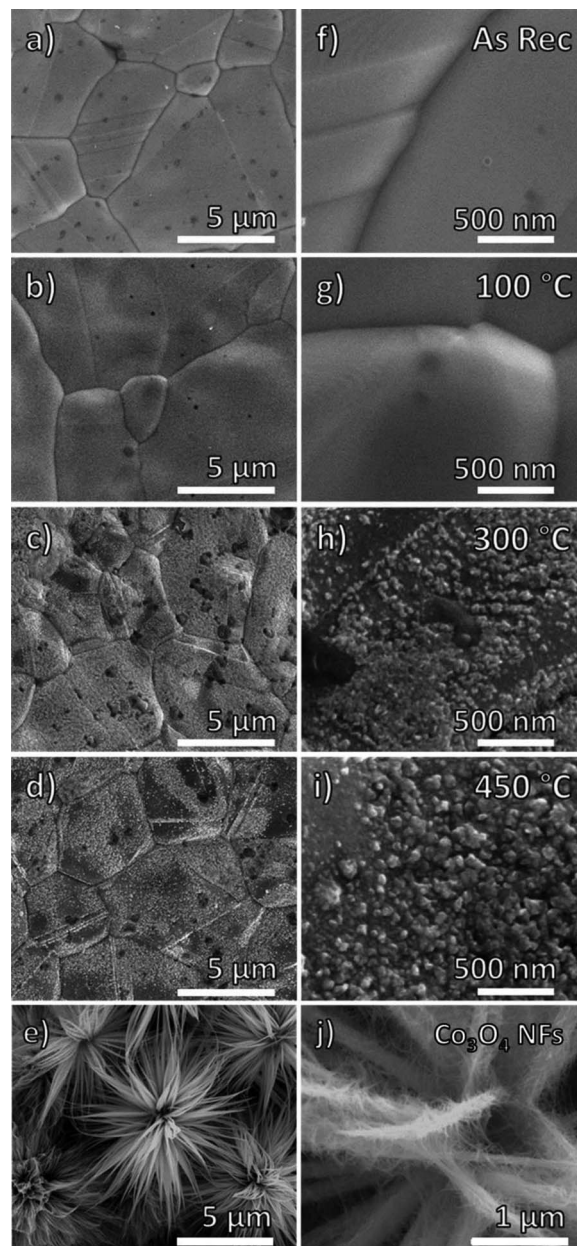


**Figure 3.** SEM images of the various Ni foam samples. Low magnification images of (a) as received Ni foam, Ni foam heated to (b) 100 °C, (c) 300 °C and (d) 450 °C and (e) Co<sub>3</sub>O<sub>4</sub> NFs prepared on Ni foam and corresponding high magnification images (f)-(j) respectively.

Co<sub>3</sub>O<sub>4</sub> arranged in a flower-like morphology. The branches of the Ni foam are heavily decorated with Co<sub>3</sub>O<sub>4</sub> NFs, as can be seen in Figure S2a,d.

A comparison of cyclic voltammograms acquired for as received and heat treated Ni foam samples and a Co<sub>3</sub>O<sub>4</sub> NF sample prepared on Ni foam are presented in Figure 4. Two cathodic peaks were observed in the first scan for the as received Ni foam at 1.09 and 0.53 V respectively. These peaks shift to 0.82 and 0.54 V in the subsequent cycles. Two peaks can be seen in the first anodic scan at 1.03 V and 2.24 V, respectively. The anodic peak at 1.03 V can be seen in the 5<sup>th</sup> and the 10<sup>th</sup> cycles. When the Ni foam was heated to 100 °C the first cathodic peak remained at 1.09 V and the second peak shifted to 0.43 V. This slight shift in potential may be associated with an increase in NiO on the surface of the Ni foam. A strong cathodic peak was observed at 0.59 V in the first scan for the Ni foam sample heated to 300 °C. The anodic peaks for the Ni foam heated to 300 °C occur at the

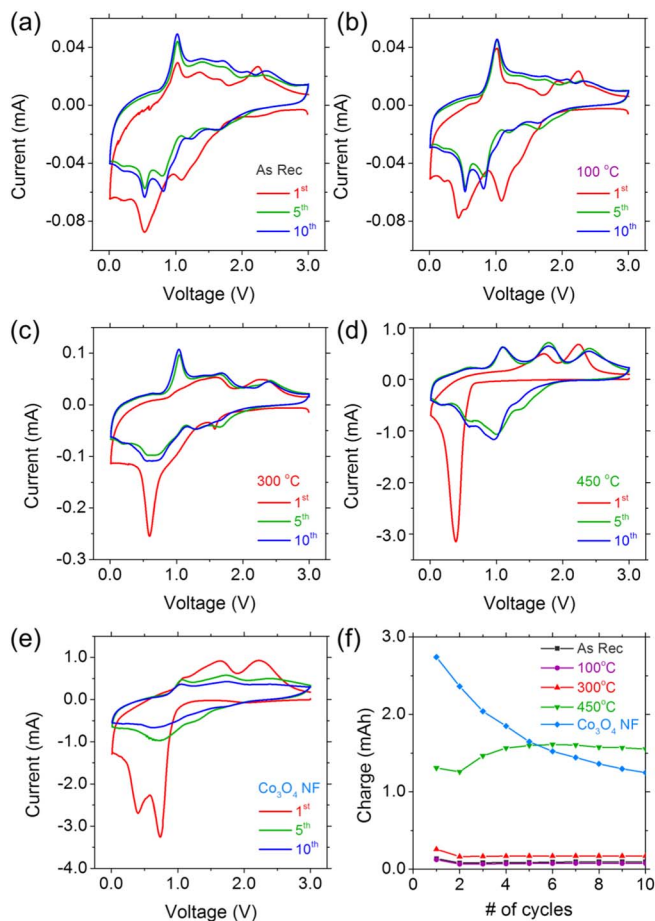


**Figure 4.** Cyclic voltammograms for (a) as received Ni foam, Ni foam heated to (b) 100°C, (c) 300°C and (d) 450°C and (e) Co<sub>3</sub>O<sub>4</sub> NFs prepared on Ni foam acquired at a scan rate of 0.2 mV s<sup>-1</sup>. (f) Comparison of charge values for as received Ni foam, heated Ni foam samples and Co<sub>3</sub>O<sub>4</sub> NFs prepared on Ni foam, calculated from cyclic voltammograms.

same potentials as the anodic peaks for as received Ni foams and Ni foam sample heated to 100°C. The Ni foam sample heated to 450°C had a strong cathodic peak at 0.38 V in the first scan. It has previously been reported for various NiO nanostructures that a strong peak in the first cathodic scan in the range of from 0.3 to 0.9 V corresponds to the initial reduction of NiO to metallic Ni and the formation of amorphous Li<sub>2</sub>O and the SEI layer.<sup>47,48</sup> Two peaks in the initial anodic scan at 1.72 and 2.24 V are associated with the formation of NiO and the decomposition of Li<sub>2</sub>O and the SEI layer.<sup>49</sup> In subsequent cycles the cathodic peak shifted to ~0.97 V. As previously discussed, NiO is a conversion mode material, i.e. during the first cathodic scan, NiO is reduced to metallic Ni. During the initial anodic scan Ni is oxidized to reform NiO. It has previously been reported that the resultant NiO nanoparticles may have quite small diameters (<5 nm).<sup>33,50</sup> The shift in the potential for the cathodic peak may be due to this reduced particle size after the first complete scan.<sup>51</sup>

The first CV scan for each sample is overlaid in Figure S3. It is clear that the measured current values of the initial cathodic peak for the as received Ni foam and the Ni foam heated to 100°C are quite low (<-0.1 mA). There is a slight increase in the measured current for the Ni foam heated to 300°C (<-0.3 mA), however the most significant increase occurs after heating the Ni foam to 450°C. The CV scans for the Ni foam sample heated to 450°C are in close agreement with previous reports on various NiO nanostructures,<sup>52,53</sup> indicating that there is a significant amount of NiO present on the surface of the foam after heating. This is also in close agreement with the XRD results shown in Figure 1.

Two strong cathodic peaks were observed in the first scan for the Co<sub>3</sub>O<sub>4</sub> NFs prepared on Ni foam at 0.74 and 0.38 V, as shown in Figure 4e. The first peak at 0.74 V is associated with the initial reduction of Co<sub>3</sub>O<sub>4</sub> to metallic Co.<sup>54,55</sup> The second peak at 0.38 V occurs at the same potential as the NiO reduction peak observed for the Ni foam sample which was heated to 450°C. From Figure 4e it is clear that the charge associated with the NiO reduction is comparable to the charge associated with the Co<sub>3</sub>O<sub>4</sub> reduction. This has a profound effect on the electrochemical characterization of materials which are prepared at high temperatures (>450°C) on Ni foam. As previously mentioned, electrode materials which are prepared on Ni foam are quite common. Here we systematically show that the contribution of an oxide layer on the surface of the Ni foam is non-trivial. Ignoring the contributions to stored charge due to the reduction of NiO can lead to a misinterpretation of CV analysis and can result in inflated capacity values for materials prepared on Ni foam. These characteristics are demonstrated for reactions specific to Li-ion batteries, as the response in aqueous capacitor-type electrolytes is more commonly known.

The total charge stored during the cathodic scans for each Ni foam sample as well as the Co<sub>3</sub>O<sub>4</sub> NFs prepared on Ni foam are compared in Figure 4f. It is immediately clear that there is a significant increase in the charge after heating the Ni foam to 450°C. The charge stored for the as received Ni foam and Ni foam heated to 100°C were both ~0.1 mAh, indicating that there is an almost negligible capacity contribution due to lower amount of NiO which forms on the surface of the Ni foam at low temperatures. The Ni foam sample heated to 300°C exhibited slightly higher charge values (~0.3 mAh), indicating that heating to 300°C results in more of an oxide layer being formed on the surface of the Ni foam than heating to 100°C. After heating to 450°C the charge initially increased to ~1.3 mAh. The initial charge for the Co<sub>3</sub>O<sub>4</sub> NFs prepared on Ni foam was significantly higher at ~2.7 mAh, which again is due to the reduction of Co<sub>3</sub>O<sub>4</sub> to Co during the cathodic scan. A comparison of the initial charge stored for Ni foam heated to 450°C and the Co<sub>3</sub>O<sub>4</sub> NFs prepared on Ni foam suggests that ~47.7% of the initial charge stored for the NFs may be due to the presence of the NiO nanoparticles formed on the Ni foam during annealing, assuming that a similar amount of NiO is formed on the surface of the Ni foam during annealing with and without the Co<sub>3</sub>O<sub>4</sub> NF precursor present.

The galvanostatic charge and discharge curves for the 1<sup>st</sup>, 25<sup>th</sup> and 50<sup>th</sup> cycles for Ni foam samples heated to various temperatures and Co<sub>3</sub>O<sub>4</sub> NFs prepared on Ni foam are shown in Figure 5. As can be seen in Figures 5a, 5b the charge stored in the initial charge for the as received Ni foam and the foam heated to 100°C are quite low, having values of 0.058 and 0.043 mAh, respectively. Upon heating to 300°C the Ni foam has the typical charge characteristics of NiO with a long voltage plateau occurring at ~0.60 V, as shown in Figure 5c.<sup>56,57</sup> This implies that there is a significant layer of NiO on the surface of the Ni foam after heating to 300°C. The initial charge (~0.233 mAh) is also higher than the initial charges for Ni foam samples heated to lower temperatures. There is a significant increase in the stored charge for the Ni foam sample heated to 450°C, as can be seen in Figure 5d. The initial charge had a value of ~1.325 mAh, which is a substantial increase compared to the Ni foam sample heated to 300°C. This again confirms that heating Ni foam to 450°C results in formation of a significant oxide layer on the surface of the Ni foam which can store a considerable amount of charge. The flat plateau observed in the first charge profile for the Ni foam samples after heating to 300 and 450°C is not seen in subsequent cycles. As discussed in the CV analysis, this may be due to the formation of nanoparticles of NiO after the first cycle which are significantly smaller than the initial NiO nanoparticles which were formed on the surface of the NiO after heating. The voltage profiles for the first charge and discharge for each sample are overlaid in Figure S4. It is immediately clear that Ni foam heated to 450°C initially stores a substantial amount of charge.

The charge and discharge profiles for Co<sub>3</sub>O<sub>4</sub> NFs are shown in Figure 5e. The plateau in the initial charge curve which begins at ~0.90 V is characteristic of Co<sub>3</sub>O<sub>4</sub>.<sup>5,58,59</sup> However this is typically a long flat plateau instead of the sloped plateau observed in

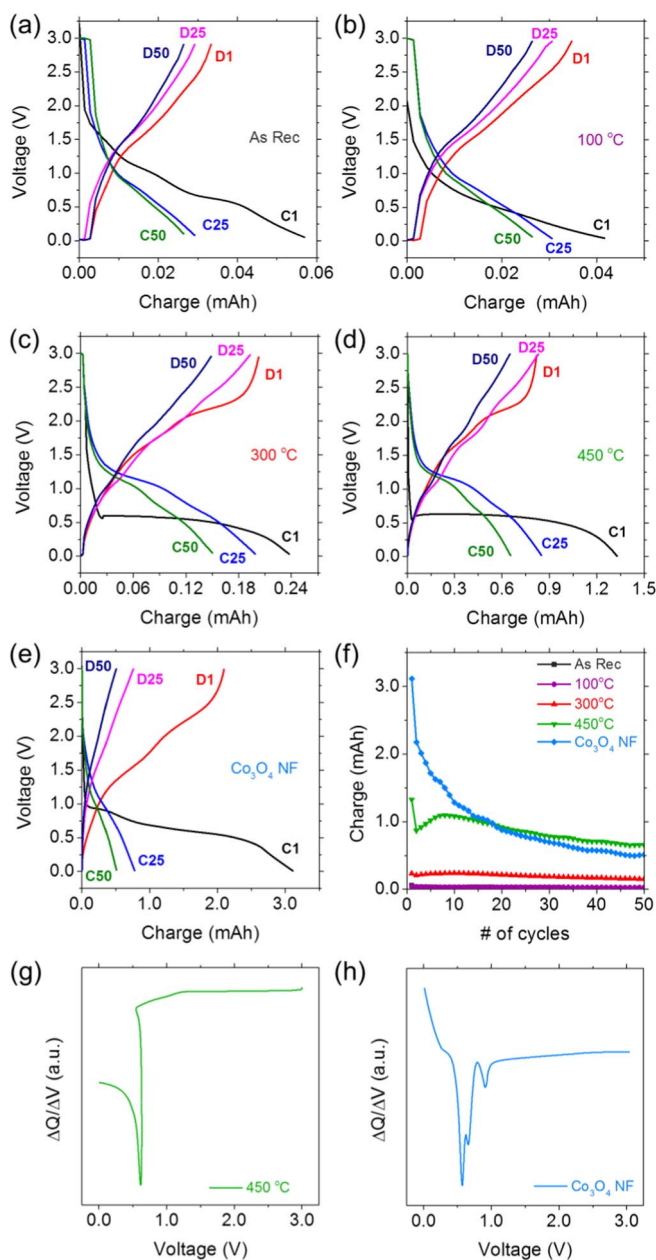


**Figure 5.** Charge and discharge voltage profiles for the 1<sup>st</sup>, 25<sup>th</sup> and 50<sup>th</sup> cycle for (a) as received Ni foam, Ni foam heated to (b) 100°C, (c) 300°C and (d) 450°C and (e) Co<sub>3</sub>O<sub>4</sub> NFs prepared on Ni foam at a constant current of  $\pm 500 \mu\text{A}$  in a potential window of 3.0–0.01 V. (f) Comparison of charge values for as received Ni foam, heated Ni foam samples and Co<sub>3</sub>O<sub>4</sub> NFs prepared on Ni foam, calculated from galvanostatic testing. Differential charge plot of the 1<sup>st</sup> galvanostatic charge curve for (g) Ni foam heated to 450°C and (h) Co<sub>3</sub>O<sub>4</sub> NFs prepared on Ni foam.

Figure 5e. To further investigate the cause of this sloped plateau, differential charge plots were calculated for the first galvanostatic charge curve for Ni foam heated to 450°C and Co<sub>3</sub>O<sub>4</sub> NFs prepared on Ni foam; these plots are presented in Figures 5g and 5h respectively. One strong peak can be seen in the differential plot for Ni foam heated to 450°C at  $\sim 0.60$  V, corresponding to the long voltage plateau which occurs at the same potential in the first galvanostatic charge curve in Figure 5d. Three peaks can be seen in the differential charge curve for Co<sub>3</sub>O<sub>4</sub> NFs prepared on Ni foam at  $\sim 0.90$ , 0.65 and 0.58 V. The first peak corresponds to the reduction of Co<sub>3</sub>O<sub>4</sub> to Co and the initial plateau which occurs at the same potential and can be seen in the first

charge curve in Figure 5e. The second and third peaks correspond to the reduction of NiO and the flat voltage profile observed in the first charge profile for the Ni foam sample heated to 450°C. The peak observed at 0.58 V is in close agreement with the peak observed at 0.60 V in the differential charge curve for Ni foam heated to 450°C. From analysis of the differential charge curves it is most likely that the initial galvanostatic charge curve for Co<sub>3</sub>O<sub>4</sub> NFs prepared on Ni foam is a convolution of the voltage response for the reduction of Co<sub>3</sub>O<sub>4</sub> to Co and NiO to Ni. This suggests that the heated Ni foam current collector is not passive during electrochemical testing. In fact, the contribution of the oxide layer which forms on the surface of the Ni foam during heating to 450°C is quite significant.

A comparison of the charge values obtained for heated Ni foam samples as well as Co<sub>3</sub>O<sub>4</sub> NFs prepared on Ni foam is shown in Figure 5f. The charge values obtained for the as received Ni foam and the Ni foam heated to 100°C were quite low ( $\sim 0.03$  mAh). Heating the Ni foam to 300°C resulted in slightly increased charge values of ( $\sim 0.20$  mAh). It is again clear that heating the Ni foam to 450°C has a significant effect on its electrochemical performance. The initial charge value for Ni foam was  $\sim 1.35$  mAh, this value decreased to  $\sim 0.85$  mAh after 25 cycles and  $\sim 0.66$  mAh after 50 cycles. The initial charge value of  $\sim 3.11$  mAh for the Co<sub>3</sub>O<sub>4</sub> NFs prepared on Ni foam was significantly higher than the Ni foam heated to 450°C. This value decreased to  $\sim 0.78$  mAh after 25 cycles and  $\sim 0.51$  mAh after 50 cycles. Comparing the initial charge stored for Ni foam heated to 450°C and the Co<sub>3</sub>O<sub>4</sub> NFs prepared on Ni foam indicates that  $\sim 42.5\%$  of the initial charge stored for the NFs may be due to the presence of the layer of NiO formed on the Ni foam during annealing, this is in close agreement with the charge contribution determined from CV analysis ( $\sim 47.7\%$ ). After the first 20 cycles the charge values for NiO heated to 450°C were slightly higher than the charge values obtained for the Co<sub>3</sub>O<sub>4</sub> NFs, indicating that the current collector may dominate the response over extended cycling. The reduction in charge stored may be due to the fact that both NiO and Co<sub>3</sub>O<sub>4</sub> are conversion mode materials. During charging both materials are reduced to their metallic forms and are then oxidized upon discharging. The significant structural changes which occur as a result of this redox process may result in the reduction in Co<sub>3</sub>O<sub>4</sub> NFs adhesion and loss electrical contact with the Ni foam.

The comparison of the charge values obtained over 50 cycles, along with the CV analysis presented in Figure 4, confirms that the layer of NiO on the surface of the Ni foam heated to 450°C is actively storing charge during cycling. Ni foam which has been heated to high temperatures is not a passive current collector.

When electrode materials are prepared on Ni foam by heating to high temperatures it is critical to consider the charge contribution from the layer of NiO present on the surface of the Ni foam. If only the added mass of the material grown on the foam is considered when determining specific capacity values, the calculated capacity values will be artificially inflated if any given mass loading does not entirely cover the NiO to prevent it from participating in the electrochemical response. It is important to recognize the effect of heating current collectors (in this case Ni foam due to the formation of the electrochemically active conversion mode anode material NiO) on the overall performance of the cells being investigated so that inaccurate values are not reported in the literature. The main findings of the study are summarized schematically in Figure 6.

## Conclusions

There are numerous reports investigating binder free anode materials which were prepared directly on Ni foam. The preparation methods for these materials are typically a two-step process, involving a hydrothermal treatment followed by a high temperature oxidation step. Through structural analysis of as received Ni foam and foam samples heated to various temperatures we have systematically shown that heating Ni foam resulted in a gradual increase in the amount of NiO formed on the surface of the Ni foam. The most significant increase occurred when the Ni foam was heated to 450°C. SEM images

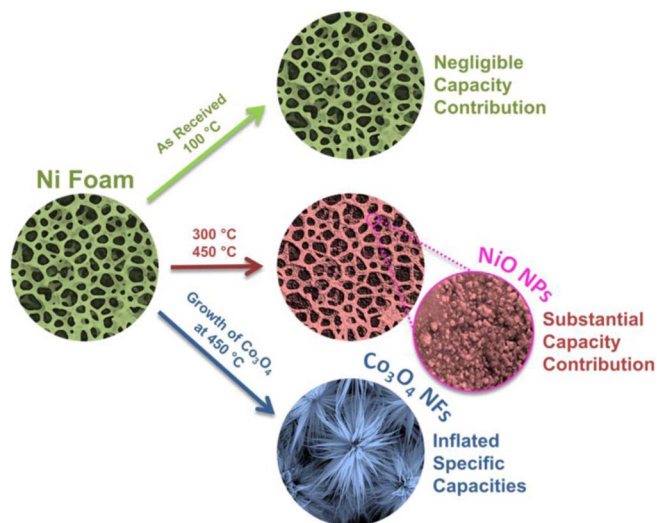


**Figure 6.** Schematic representation of the effects of heat-treatment on Ni foam.

demonstrate that Ni foam heated to 450°C was decorated with NiO nanoparticles. XRD analysis confirmed that the layer of nanoparticles is composed of cubic NiO. Cyclic voltammetry and galvanostatic tests of heated Ni foam samples demonstrated that the total charge stored for as received foam and the foam heated to 100°C was quite low (~0.1 mAh). This suggests that the capacity contribution due to the inherent surface chemistry of the foam samples at low temperatures is almost negligible. Heating the Ni foam to 300°C results in a greater amount of NiO being formed and consequently there is a slight increase in the total stored charge.

Heating the Ni foam to 450°C results in a significant increase in the charge stored compared to the Ni foam samples heated to lower temperatures. The electrochemical response of Ni foam samples heated to 450°C is in close agreement with previous reports on NiO nanostructures, indicating that a significant amount of NiO is formed on the surface of the Ni foam. The initial charge value for Ni foam heated to 450°C was ~1.35 mAh, confirming that the layer of NiO on the surface of the Ni foam is actively storing charge during cycling. The electrochemical analysis of heated Ni foam samples confirms that contribution of the resultant layer of NiO toward the stored charge is substantial. This has significant consequences for electrode materials which are prepared directly on Ni foam.

To further investigate this, Co<sub>3</sub>O<sub>4</sub> NFs were prepared on Ni foam via a hydrothermal treatment followed by an oxidation step via annealing at 450°C. Through comparison of cyclic voltammetry for bare Ni foam heated to 450°C and the Co<sub>3</sub>O<sub>4</sub> NFs it was clear that the layer of NiO had a significant contribution toward the stored charge. Discrete cathodic peaks due to the reduction of NiO were clearly visible in the CV scans for Co<sub>3</sub>O<sub>4</sub> NFs prepared on Ni foam. Through electrochemical analysis we have systematically shown that the contribution of NiO which forms on the surface of Ni foam when heated is non-negligible. When electrode materials are prepared on Ni foam via a high temperature oxidation process the contribution of the layer of NiO toward the stored charge should not be ignored.

#### Acknowledgments

This work was supported by a Science Foundation Ireland Technology Innovation and Development Awards under contract no. 13/TIDA/E2761. This research has received funding from the Seventh Framework Programme FP7/2007-2013 (Project STABLE) under grant agreement no. 314508. This publication has also emanated from research supported in part by a research grant from SFI under grant Number 14/IA/2581.

#### References

- V. Etacheri, R. Marom, R. Elazari, G. Salitra, and D. Aurbach, *Energy Environ. Sci.*, **4**, 3243 (2011).
- B. Scrosati, J. Hassoun, and Y.-K. Sun, *Energy Environ. Sci.*, **4**, 3287 (2011).
- B. Scrosati and J. Garche, *J. Power Sources*, **195**, 2419 (2010).
- T. Kennedy, M. Brandon, and K. M. Ryan, *Adv. Mater.* (2016).
- D. McNulty, H. Geaney, E. Armstrong, and C. O'Dwyer, *J. Mater. Chem. A*, **4**, 4448 (2016).
- D. McNulty, D. N. Buckley, and C. O'Dwyer, *J. Electrochem. Soc.*, **161**, A1321 (2014).
- D. McNulty, D. N. Buckley, and C. O'Dwyer, *J. Solid State Electrochem.*, **20**, 1445 (2016).
- C. Zhang, H. Song, C. Liu, Y. Liu, C. Zhang, X. Nan, and G. Cao, *Adv. Funct. Mater.*, **25**, 3497 (2015).
- L. Hu, H. Wu, F. La Mantia, Y. Yang, and Y. Cui, *ACS Nano*, **4**, 5843 (2010).
- G. Tan, F. Wu, C. Zhan, J. Wang, D. Mu, J. Lu, and K. Amine, *Nano Lett.*, **16**, 1960 (2016).
- D. McNulty, D. N. Buckley, and C. O'Dwyer, *J. Power Sources*, **267**, 831 (2014).
- P. K. Nayak, J. Grinblat, M. D. Levi, O. Haik, E. Levi, M. Talianker, B. Markovsky, Y.-K. Sun, and D. Aurbach, *Chem. Mater.*, **27**, 2600 (2015).
- E. Armstrong, D. McNulty, H. Geaney, and C. O'Dwyer, *ACS Appl. Mater. Interfaces*, **7**, 27006 (2015).
- H. Wu, G. Yu, L. Pan, N. Liu, M. T. McDowell, Z. Bao, and Y. Cui, *Nat. Commun.*, **4** (2013).
- X. Li, M. Gu, S. Hu, R. Kennard, P. Yan, X. Chen, C. Wang, M. J. Sailor, J.-G. Zhang, and J. Liu, *Nat. Commun.*, **5** (2014).
- H. Wu, G. Chan, J. W. Choi, I. Ryu, Y. Yao, M. T. McDowell, S. W. Lee, A. Jackson, Y. Yang, L. Hu, and Y. Cui, *Nat. Nanotechnol.*, **7**, 310 (2012).
- A. K. Manohar, S. Malkhandi, B. Yang, C. Yang, G. K. Surya Prakash, and S. R. Narayanan, *J. Electrochem. Soc.*, **159**, A1209 (2012).
- H. Geaney, J. O'Connell, J. D. Holmes, and C. O'Dwyer, *J. Electrochem. Soc.*, **161**, A1964 (2014).
- P. L. Taberna, S. Mitra, P. Poizot, P. Simon, and J. M. Tarascon, *Nat. Mater.*, **5**, 567 (2006).
- H. Long, T. Shi, S. Jiang, S. Xi, R. Chen, S. Liu, G. Liao, and Z. Tang, *J. Mater. Chem. A*, **2**, 3741 (2014).
- D. McNulty, D. N. Buckley, and C. O'Dwyer, *ECS Trans.*, **50**, 165 (2013).
- H.-C. Wu, H.-C. Wu, E. Lee, and N.-L. Wu, *Electrochem. Commun.*, **12**, 488 (2010).
- Y. Luo, J. Luo, J. Jiang, W. Zhou, H. Yang, X. Qi, H. Zhang, H. J. Fan, D. Y. W. Yu, C. M. Li, and T. Yu, *Energy Environ. Sci.*, **5**, 6559 (2012).
- J. Jiang, J. Liu, R. Ding, X. Ji, Y. Hu, X. Li, A. Hu, F. Wu, Z. Zhu, and X. Huang, *J. Phys. Chem. C*, **114**, 929 (2010).
- Y. Wang, H. Xia, L. Lu, and J. Lin, *ACS Nano*, **4**, 1425 (2010).
- Z. Li, H. Zhao, J. Wang, P. Lv, Z. Zhang, Z. Zeng, and Q. Xia, *Electrochim. Acta*, **182**, 398 (2015).
- W. Chen, S. Maloney, and W. Wang, *Electrochim. Acta*, **176**, 96 (2015).
- X. Zhou, G. Chen, J. Tang, Y. Ren, and J. Yang, *J. Power Sources*, **299**, 97 (2015).
- N. Padmanathan, H. Shao, D. McNulty, C. O'Dwyer, and K. M. Razeed, *J. Mater. Chem. A*, **4**, 4820 (2016).
- S. Ni, X. Lv, T. Li, X. Yang, and L. Zhang, *J. Mater. Chem. A*, **1**, 1544 (2013).
- S. Ni, T. Li, X. Lv, X. Yang, and L. Zhang, *Electrochim. Acta*, **91**, 267 (2013).
- S. A. Needham, G. X. Wang, and H. K. Liu, *J. Power Sources*, **159**, 254 (2006).
- P. Poizot, S. Laruelle, S. Grugeon, L. DuPont, and J. Tarascon, *Nature*, **407**, 496 (2000).
- H. Liu, G. Wang, J. Liu, S. Qiao, and H. Ahn, *J. Mater. Chem.*, **21**, 3046 (2011).
- X. P. Gao, J. L. Bao, G. L. Pan, H. Y. Zhu, P. X. Huang, F. Wu, and D. Y. Song, *J. Phys. Chem. B*, **108**, 5547 (2004).
- J. C. Park, J. Kim, H. Kwon, and H. Song, *Adv. Mater.*, **21**, 803 (2009).
- G. Zhou, D.-W. Wang, F. Li, L. Zhang, N. Li, Z.-S. Wu, L. Wen, G. Q. Lu, and H.-M. Cheng, *Chem. Mater.*, **22**, 5306 (2010).
- X. Li, A. Dhanabalan, K. Bechtold, and C. Wang, *Electrochem. Commun.*, **12**, 1222 (2010).
- A. Kvasha, E. Azaceta, O. Leonet, M. Bengochea, I. Boyano, R. Tena-Zaera, I. de Meaza, O. Miguel, H.-J. Grande, and J. A. Blazquez, *Electrochim. Acta*, **180**, 16 (2015).
- T. K. Kim, X. Li, and C. Wang, *Appl. Surf. Sci.*, **264**, 419 (2013).
- H.-C. Wu, E. Lee, N.-L. Wu, and T. R. Jow, *J. Power Sources*, **197**, 301 (2012).
- T. K. Kim, W. Chen, and C. Wang, *J. Power Sources*, **196**, 8742 (2011).
- L. Leng, X. Zeng, H. Song, T. Shu, H. Wang, and S. Liao, *J. Mater. Chem. A*, **3**, 15626 (2015).
- M. Grdeń, M. Alsabet, and G. Jerkiewicz, *ACS Appl. Mater. Interfaces*, **4**, 3012 (2012).
- K. S. Kim and N. Winograd, *Surf. Sci.*, **43**, 625 (1974).
- D. Lee, S. Yoon, D. Yoon, and S. Suh, *J. Korean Phys. Soc.*, **44**, 1079 (2004).
- X. Wang, X. Li, X. Sun, F. Li, Q. Liu, Q. Wang, and D. He, *J. Mater. Chem.*, **21**, 3571 (2011).
- E. Hosono, S. Fujihara, I. Honma, and H. Zhou, *Electrochem. Commun.*, **8**, 284 (2006).
- X. H. Huang, J. P. Tu, B. Zhang, C. Q. Zhang, Y. Li, Y. F. Yuan, and H. M. Wu, *J. Power Sources*, **161**, 541 (2006).
- X. Li, A. Dhanabalan, and C. Wang, *J. Power Sources*, **196**, 9625 (2011).
- B. Varghese, M. V. Reddy, Z. Yanwu, C. S. Lit, T. C. Hoong, G. V. Subba Rao, B. V. R. Chowdari, A. T. S. Wee, C. T. Lim, and C.-H. Sow, *Chem. Mater.*, **20**, 3360 (2008).
- J.-H. Jang, B.-M. Chae, H.-J. Oh, and Y.-K. Lee, *J. Power Sources*, **304**, 189 (2016).

53. L. Gu, W. Xie, S. Bai, B. Liu, S. Xue, Q. Li, and D. He, *Appl. Surf. Sci.*, **368**, 298 (2016).
54. H.-C. Liu and S.-K. Yen, *J. Power Sources*, **166**, 478 (2007).
55. Z.-S. Wu, W. Ren, L. Wen, L. Gao, J. Zhao, Z. Chen, G. Zhou, F. Li, and H.-M. Cheng, *ACS Nano*, **4**, 3187 (2010).
56. S. Hao, B. Zhang, S. Ball, B. Hu, J. Wu, and Y. Huang, *Mater. Des.*, **92**, 160 (2016).
57. M. A. Rahman and C. Wen, *Ionics*, **21**, 2709 (2015).
58. Y. Li, B. Tan, and Y. Wu, *Nano Lett.*, **8**, 265 (2008).
59. Y.-M. Kang, M.-S. Song, J.-H. Kim, H.-S. Kim, M.-S. Park, J.-Y. Lee, H. K. Liu, and S. X. Dou, *Electrochim. Acta*, **50**, 3667 (2005).